Sensors and Materials, Vol. 27, No. 10 (2015) 907–915
MYU Tokyo

S & M 1127

Structural and Optical Characterizations of ZnO Nanowire Arrays Grown on Si Substrate

Takeshi Ishiyama*, Tsutomu Fujii and Takaya Nakane

Department of Electrical and Electronic Information Engineering, Toyohashi University of Technology, 1-1 Hibarigaoka, Tempaku-cho, Toyohashi, Aichi 441-8580, Japan

(Received February 13, 2015; accepted June 24, 2015)

Key words: zinc oxide, silicon, nanowire, vapor-liquid-solid process, ultraviolet luminescence

Arrays of single-crystal zinc oxide (ZnO) nanowires have been synthesized on silicon substrates by vapor-liquid-solid growth techniques. The effects of growth conditions including substrate temperature and Ar gas flow rate on the growth properties of ZnO nanowire arrays were studied. Structural and optical characterization was performed using scanning electron microscopy (SEM) and photoluminescence (PL) spectroscopy. SEM images of the ZnO nanowire arrays grown at various Ar gas flow rates indicated that the alignment and structural features of ZnO nanowires were affected by the gas flow rate. The PL of the ZnO nanowire arrays exhibited a strong ultraviolet (UV) emission at 380 nm and a weak green emission at around 510 nm. A blue shift and broadening of the UV emission were observed with an increase in Ar gas flow rate.

1. Introduction

Zinc oxide (ZnO) semiconductor materials are currently attracting considerable attention, as evident from the large increase in the number of recent publications. ZnO is regarded as a promising candidate material for ultraviolet (UV) light-emitting diodes[1,2] and laser devices[4–6] because of its relatively large exciton binding energy of 60 meV and wide direct band gap of 3.37 eV at room temperature. The optoelectronic applications of ZnO overlap those of gallium nitride (GaN), which has a bandgap of 3.4 eV at room temperature and is widely used for the production of green, blue-UV, and white light-emitting devices. However, ZnO has advantages over GaN in terms of the availability of high-quality bulk single crystals and having a large exciton binding energy of 60 meV. In addition, ZnO can be grown by simple crystal-growth technologies, potentially lowering the costs of ZnO-based devices. Recently, ZnO nanostructures have been extensively studied owing to their unique applications in mesoscopic physics and chemistry. The properties of ZnO nanostructures strongly depend on both their size and shape. The ability to easily manipulate the structure and morphology of ZnO has led to particular

*Corresponding author: e-mail: ishiyama@ee.tut.ac.jp

ISSN 0914-4935

interest in its nanostructures. A wide variety of nanoscale morphologies can be grown, such as wires, rods, tetrapods, belts, rings, and combs.[7–11] In particular, ZnO nanowires and nanorods grown by vapor deposition techniques and solution-based methods have attracted interest because of their possible applications in optoelectronic devices, such as light-emitting diodes, transparent field-effect transistors, UV light detectors, and solar cells. The fabrication of nanoscale devices has become the focus of intensive research in the area of photonics.[12–22] ZnO nanowires grown on Si substrates are well suited for the development of such optoelectronic devices. Specific applications include the use of n-ZnO/p-Si heterostructure photodiodes for UV and visible light detection.[23–25] Metal-catalyst-assisted thermal chemical vapor transport via the vapor-liquid-solid (VLS) mechanism is a popular technique for fabricating ZnO nanowires on Si substrates. The synthesis of well-aligned ZnO nanowire arrays is highly important for the fabrication of optoelectronic devices. There are a number of reports of ZnO VLS nanowire growth.[26–33] However, the effect of growth conditions on the resulting ZnO nanowires and their growth mechanisms remain unclear. A comprehensive understanding of nanowire growth is important for controling the synthesis of nanowires.

In this paper, we report on the structural and optical characterization of ZnO nanowires grown on Si substrates by VLS growth methods. In particular, the effect of the gas flow rate on the structural features of ZnO nanowire arrays is examined. The alignment and structural features of ZnO nanostructures are strongly affected by the gas flow rate. Scanning electron microscopy (SEM) images of the ZnO nanostructures reveal well-aligned nanowire arrays. Beltlike and comblike structures are observed in the samples grown at high gas flow rates. The photoluminescence (PL) of the ZnO nanowires on Si exhibited a strong UV emission at 380 nm and a weak green emission at approximately 510 nm. A blue shift in the UV emission was observed in the samples grown under an Ar gas flow.

2. Experimental Techniques

The synthesis of ZnO nanowire arrays on a Si substrate was carried out by conventional Au-catalyst-assisted thermal chemical vapor transport, as schematically shown in Fig. 1. The source material was a mixture of zinc (II) oxide powder (99.999%) and graphite powder (99.9%) at a ratio of 2:1 by weight. The source material and a Au-covered Si substrate were placed in a quartz tube. The Si substrates were cut from a (111)-oriented Czochralski (CZ) Si wafer. Chemical etching of the Si wafer surface was carried out in a mixed acid solution with 5% HF. Then a layer of Au about 5 nm thick, as measured using a quartz crystal monitor, was first deposited on Si substrates by thermal vacuum evaporation. Separately, a quartz tube of 30 mm diameter was transferred into a horizontal furnace. One side of the quartz tube was connected to an Ar gas inlet and the other side to a vacuum pump. The source materials were placed at a hot zone in the center of the furnace. The Si substrate was placed downstream in the inner tube in the direction of gas flow. The natural temperature gradient of the furnace resulted in a difference in substrate temperature from 200 to 800 °C. The source material was heated at 1000 °C and was maintained under a constant flow of Ar gas for 30 min. The entire

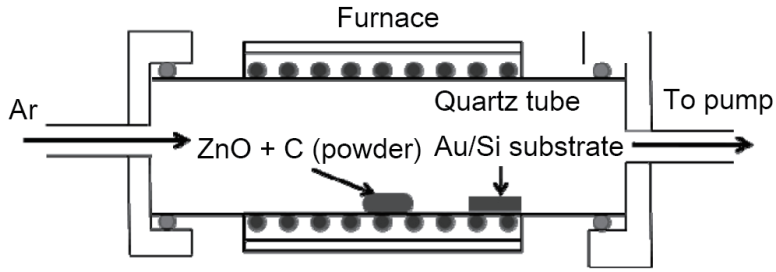

Fig. 1. Schematic diagram of the experimental apparatus for growth of ZnO nanowire arrays in horizontal quartz tube furnace by VLS.

system was evacuated to a base pressure of 40 Pa. Then Ar gas was introduced into the system at rates varying from 1 to 4 L/min. The furnace was then turned off and allowed to cool to room temperature. The surface morphology of ZnO nanowires was observed by SEM (JSM-6300). PL measurements were carried out at room temperature using the 365 nm excitation of a UV-LED (OMRON ZUV-C30H) and a miniature fiber optic spectrometer (Ocean Optics USB-2000).

3. Results and Discussion

Figures 2(a) and 2(b) show typical SEM images of the as-prepared nanowires grown under a base pressure of 40 Pa without Ar gas flow and at an Ar gas flow of 1 L/min at atmospheric pressure, respectively. The substrate temperatures were optimized to 600 °C in both cases because SEM images showed that the well-aligned nanowires were grown at the substrate temperature. It is clear that a well-aligned nanowire array was grown uniformly on the Si substrate under Ar gas flow. The nanowires were straight, smooth, and relatively vertical to the Si substrate. The substrate temperature was optimized at 600 °C in both cases. The nanowires were not synthesized well below 500 °C, and a rough morphology was observed in samples grown above 700 °C. The reaction between ZnO and C produces Zn vapor and CO gas, and the oxidation of Zn provides ZnO crystals. The main reaction is expected to be $ZnO(S) + C(S) \leftrightarrow Zn(g) + CO(g)$.[26] Energy dispersive X-ray spectroscopy (EDX) analysis of these nanowires confirmed that the elemental composition is 49.05 at.% Zn, 45.00 at.% O, 5.00 at.% Si, and 0.005 at.% Au. The room-temperature PL spectrum of the ZnO nanowire array grown at an Ar gas flow of 1 L/min is shown in Fig. 3. A UV emission band is observed at 380 nm, which corresponds to the near-bandgap-edge emission. The FWHM of the UV emission is estimated to be approximately 0.1 eV. The narrow FWHM indicates uniformity and a narrow size distribution of the ZnO nanowires.[26] A weak green emission at around 510

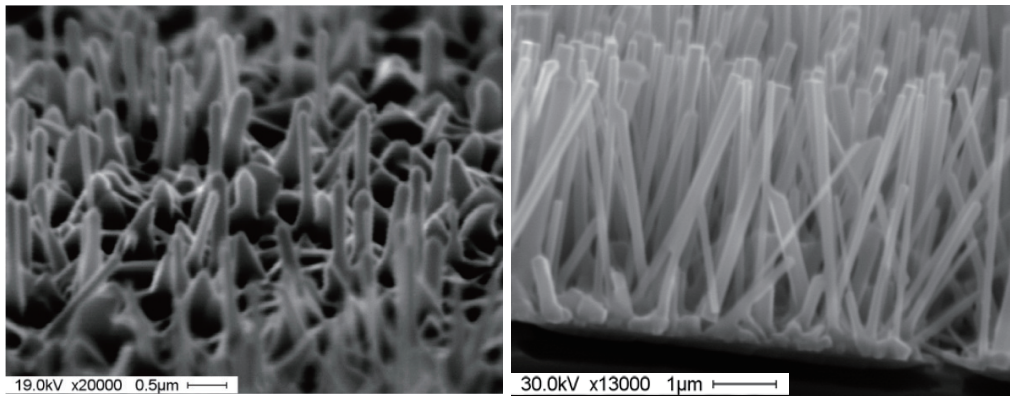

(a) (b)

Fig. 2. SEM images of ZnO nanowires grown on Si substrates under different growth conditions: (a) under a base pressure of 40 Pa without Ar gas flow and (b) ambient pressure of 0.1 MPa with Ar gas flow at 1 L/min.

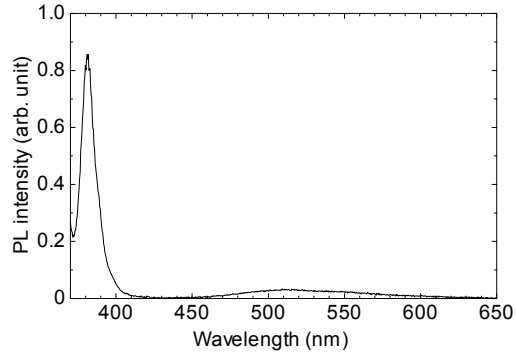

Fig. 3. PL spectrum of ZnO nanowires grown with Ar gas flow at 1 L/min.

nm is also observed, which is considered to originate from defect states such as surface defects and oxygen.[33] The ratios of the UV to visible emission intensities suggest that the crystallinity of ZnO nanowires grown with Ar gas flow was improved compared with those grown without Ar gas flow. The SEM images of ZnO nanowire arrays grown at different Ar gas flow rates are shown in Fig. 4. The substrate temperature and source heating temperature were maintained at ~600 and ~1000 °C, respectively. We confirm that the growth under Ar gas flow leads to the formation of well-aligned ZnO nanowire arrays. However, disordered nanowire arrays and belt- and comblike structures were observed at Ar gas flow rates of above 3 L/min. The diameter of nanowires decreased at higher Ar gas flow rates, as shown in Fig. 5.

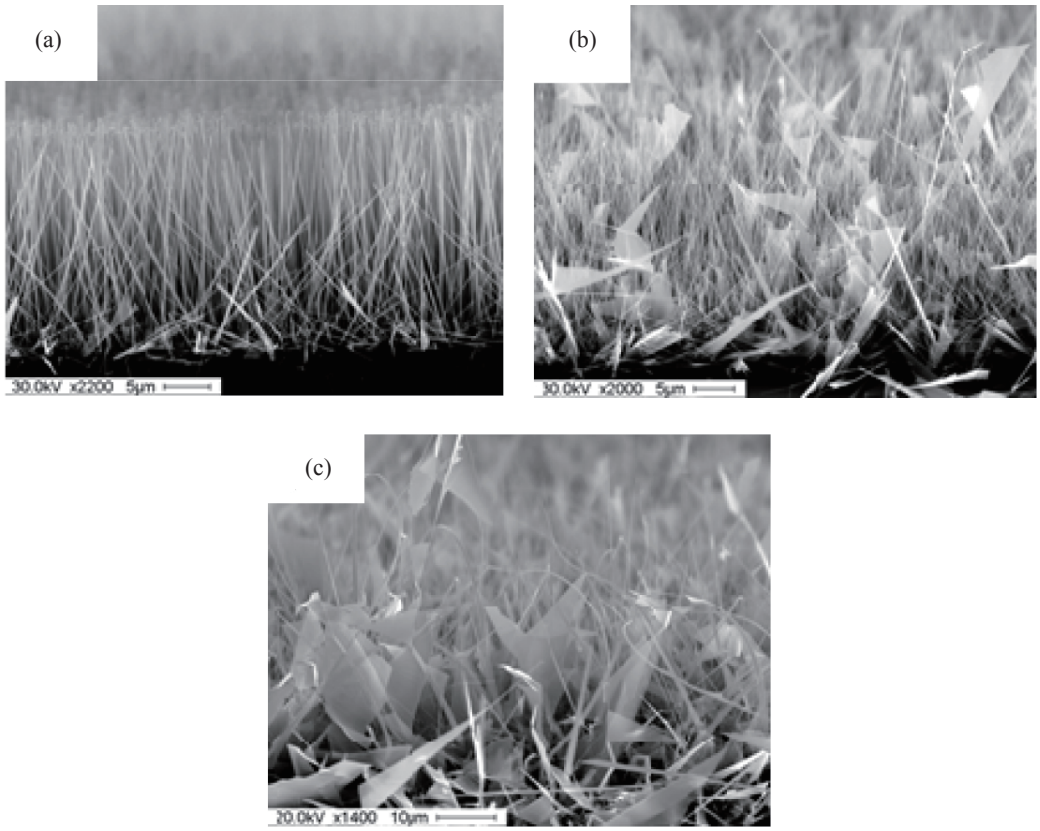

Fig. 4. SEM images of ZnO nanowires grown on Si substrates at different Ar gas flow rates: (a) 2, (b) 3, and (c) 4 L/min.

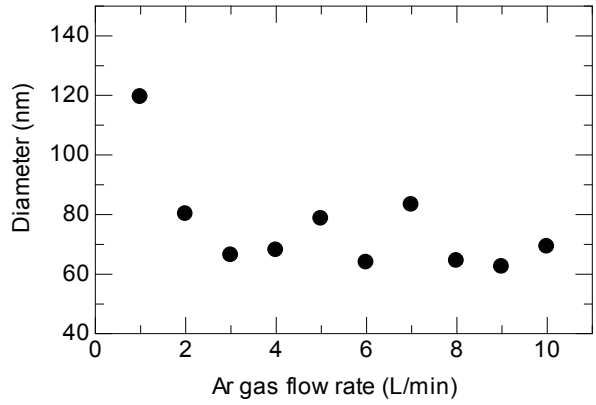

Fig. 5. Dependence of the diameter of nanowires grown on (111) Si substrate on gas flow rate.

The PL spectra in Fig. 6 show both the UV emission at 380 nm and a broad green emission at around 510 nm. By comparison, the sample grown under a base pressure of 40 Pa without Ar gas flow showed no emission spectrum. The weak green emission intensity declined at higher Ar gas flow rates, as shown in Fig. 6, and finally disappeared in the ZnO nanowire arrays grown at Ar gas flow rates above 3 L/min. Growth under Ar gas flow reduces the number of deep level defect states and improves the crystallinity of the ZnO nanowire. Disordered ZnO nanowire arrays and other structures, such as belt- and comblike structures, were observed at Ar gas flow rates above 3 L/min. A blue shift and a broadening of the UV emission are clearly observed in the PL spectra shown in Fig. 7. The peak UV emission wavelength of the samples grown at flow rates above 2 L/min is shorter than that of the sample grown at 1 L/min, suggesting a quantum confinement effect from the reduction in the nanowire diameter and formation of belt- and comb-like structures. In addition, the samples grown above 3 L/min contain a large variety of disordered nanostructures such as belt- and comblike structures, which may contribute to the broadening of the UV emission spectra.

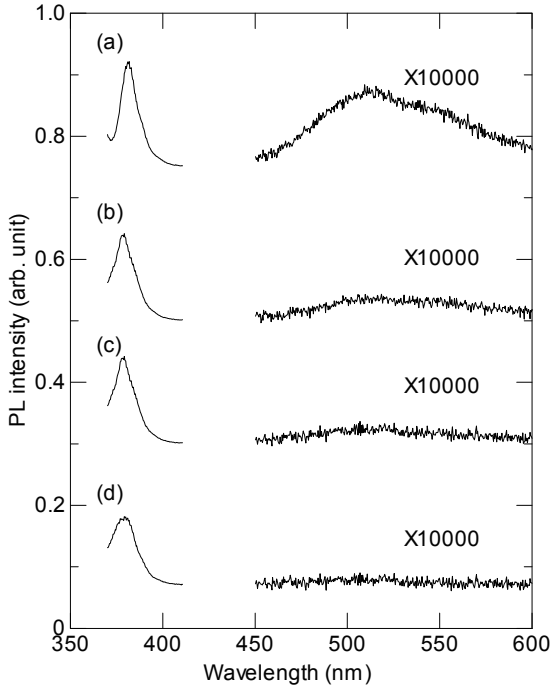

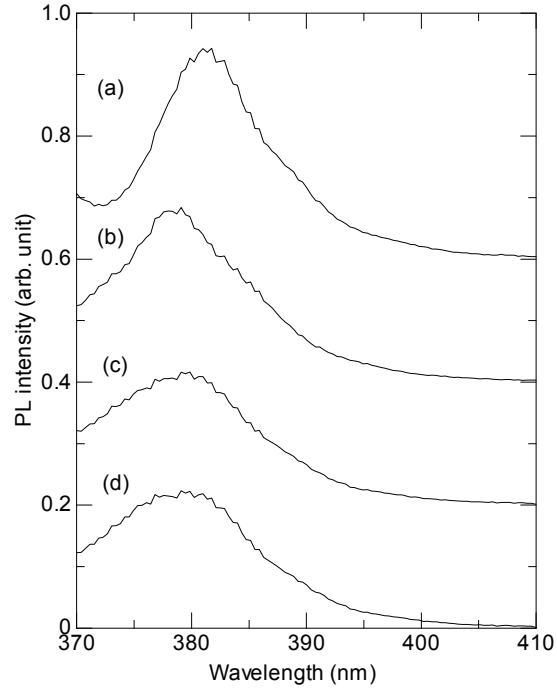

Fig. 6 (left). PL spectra of the samples grown at different Ar gas flow rates: (a) 1, (b) 2, (c) 3, and (d) 4 L/min.

Fig. 7 (right). PL spectra of UV emission in the samples grown at different Ar gas flow rates: (a) 1, (b) 2, (c) 3, and (d) 4 L/min.

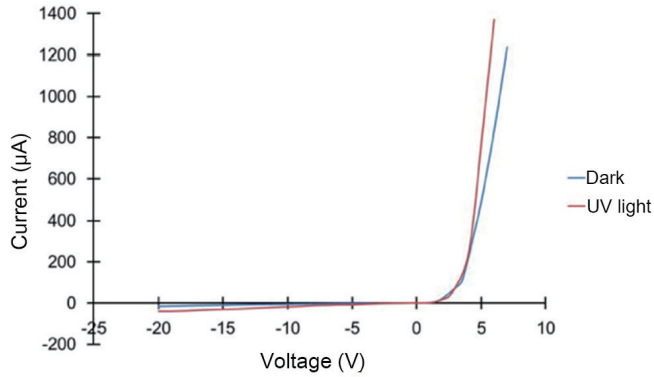

Fig. 8. (Color online) *I–V* characteristic measured under dark conditions and illuminated with UV light.

Finally, we fabricated a diode structure. The ZnO nanowires are grown on p-type Si substrate. They were covered with tin-doped indium oxide (ITO), which acts as an electrode. The ITO layer was synthesized by the spray method. A solution containing $InCl_3 \cdot 4H_2O$, $SnCl_2 \cdot 2H_2O$, and ethanol was sprayed on the substrate on which the nanowires were grown at 350 °C. After that, the sample was annealed at 600 °C for 1 h in air ambient. The current-voltage (*I–V*) characteristics of the diode were measured under dark conditions and also under illumination with UV light, as shown in Fig. 8. The *I–V* curve of the structure under dark conditions shows clear rectification with a threshold voltage of approximately 2 V and a reverse leakage current of 1 μA at a bias voltage of −3 V. Therefore, the formation of a heterogeneous p–n junction was confirmed. When UV light illumination was applied, the structure emitted photocurrent.

4. Conclusions

The structural and optical properties of ZnO nanowire arrays grown on Si substrates by VLS growth techniques have been studied. The alignment and structural features of the ZnO nanostructures were strongly affected by the Ar gas flow rate. Well-aligned nanowire arrays were observed in the samples grown at Ar gas flow rates of 1 and 2 L/min. X-ray diffraction (XRD) measurements confirmed that the nanowires had typical ZnO hexagonal wurtzite structures with the nanowires preferentially oriented along the c-axis. Various SEM images of the ZnO nanostructures revealed the formation of belt- and comblike structures in samples grown at Ar gas flow rates of 3 and 4 L/min. The PL measurements exhibited a strong UV emission at 380 nm and a weak green emission at approximately 510 nm in the samples grown under an Ar gas flow. In addition to the blue shift of the UV emission, broadening was also observed. The broadening is likely to result from an increase in the diversity of the sizes and shapes of nanostructures. In addition, the formation of a heterogeneous p–n junction was confirmed in the sample of nanowires grown on p-type Si.

Acknowledgements

This work was supported by the Kurata Memorial Hitachi Science and Technology Foundation, Public Interest TATEMATSU Foundation, and Ichihara International Scholarship Foundation.

References

1 X. M. Zhang, M.-Y. Lu, Y. Zhang, L. Chen and Z. L. Wang: Adv. Mater. **21** (2009) 2767.
2 A. Tsukazaki, A. Ohtomo, T. Onuma, M. Ohtoni, T. Makino, M. Sumina, K. Ohtani, S. F. Chichibu, S. Fuke, Y. Segawa, H. Ohno, H. Koinuma and M. Kawasaki: Nat. Mater. **4** (2005) 42.
3 J. Y. Zhang, P. J. Li, H. Sun, T. S. Deng, K. T. Zhu, Q. F. Zhang and J. L. Wu: Appl. Phys. Lett. **93** (2008) 021116.
4 J.-H. Choy, E.-S. Jang, J.-H. Won, J.-H. Chung, D.-J. Jang and Y.-W. Kim: Adv. Mater. **15** (2003) 1911.
5 R. Könenkamp, R. C. Word and M. Godinez: Nano Lett. **5** (2005) 2005.
6 Z. K. Tang, G. K. L. Wong, P. Yu, M. Kawasaki, A. Ohtomo, H. Koinuma and Y. Segawa: Appl. Phys. Lett. **72** (1998) 3270.
7 S. H. Dalal, D. L. Baptista, K. B. K. Teo, R. G. Lacerda, D. A. Jefferson and W. I. Milne: Nanotechnology **17** (2006) 4811.
8 V. A. L. Roy, A. B. Djurisic, W. K. Chan, J. Gao, H. F. Lui and C. Surya: Appl. Phys. Lett. **83** (2003) 141.
9 X. Y. Kong and Z. L. Wang: Appl. Phys. Lett. **84** (2004) 975.
10 C. S. Lao, P. X. Gao, R. S. Yang, Y. Zhang, Y. Dai and Z. L. Wang: Chem. Phys. Lett. **417** (2006) 358.
11 Z. L. Wang: J. Phys. Condens. Matter **16** (2004) 829.
12 Y. Xia, P. Yang, Y. Sun, Y. Wu, B. Mayers, B. Gates, Y. Yin, F. Kim and H. Yan: Adv. Mater. **15** (2003) 353.
13 J. Sanghyun, L. Kangho, D. B. Janes, M. H. Yoon, A. Facchetti and T. J. Marks: Nano Lett. **5** (2005) 2281.
14 Q. Ahsanulhaq, J. H. Kim and Y. B. Hahn: Nanotechnology **18** (2007) 485307.
15 K. Yubuta, T. Sato, A. Nomura, K. Haga and T. Shishido: J. Alloys Compd. **436** (2007) 396.
16 J. M. Bao, M. A. Zimmler, F. Capasso, X. W. Wang and Z. F. Ren: Nano Lett. **6** (2006) 1719.
17 O. Hayden, R. Agarwal and C. M. Lieber: Nat. Mater. **5** (2006) 352.
18 F. Qian, S. Gradecak, Y. Li, C. Y. Wen and C. M. Lieber: Nano Lett. **5** (2005) 2287.
19 D. J. Sirbuly, A. Tao, M. Law, R. Fan and P. Yang: Adv. Mater. **19** (2007) 61.
20 H. Zhou, M. Wissinger, J. Fallert, R. Hauschild, F. Stelzl, C. Klingshirn and H. Kalt: Appl. Phys. Lett. **91** (2007) 181112.
21 M. A. Zimmler, J. Bao, F. Capasso, S. Müller and C. Ronning: Appl. Phys. Lett. **93** (2008) 051101.
22 T. Voss, G. T. Svacha, E. Mazur, S. Muller, C. Ronning, D. Konjhodzic and F. Marlow: Nano Lett. **7** (2007) 3675.
23 J. D. Ye, S. L. Gu, S. M. Zhu, W. Liu, S. M. Liu, R. Zhang, Y. Shi and Y. D. Zheng: Appl. Phys. Lett. **88** (2006) 182112.
24 S. Hui, Q.-F. Zhang and J.-L. Wu: Nanotechnology **17** (2006) 2271.
25 M. A. Zimmler, T. Voss, C. Ronning and F. Capasso: Appl. Phys. Lett. **94** (2009) 241120.
26 C. Geng, Y. Jiang, Y. Yao, X. Meng, J. A. Zapien, C. S. Lee, Y. Lifshitz and S. T. Lee: Adv. Funct. Mater. **14** (2004) 589.

27 Y. H. Yang, Y. Feng and G. W. Yang: Appl. Phys. A **102** (2011) 319.
28 W. Ouyang and J. Zhu: Mater. Lett. **62** (2008) 2557.
29 L. Y. Chen, S. H. Wu and Y. T. Yin: J. Phys. Chem. C **113** (2009) 21572.
30 F. Fang, D. X. Zhao, J. Y. Zhang, D. Z. Shen, Y. M. Lu, X. W. Fan, B. H. Li and X. H. Wang: Mater. Lett. **62** (2008) 1092.
31 X. H. Wang, R. B. Li and D. H. Fan: Appl. Surf. Sci. **257** (2011) 2960.
32 R. Yousefi and A. K. Zak: Mater. Sci. Semicond. Process. **14** (2011) 170.
33 M. Rajabi, R. S. Dariani and A. Irajizad: Mater. Sci. Semicond. Process. **16** (2013) 171.